NONLINEAR ANALYSIS OF PRESSURE OSCILLATIONS IN RAMJET ENGINES

Vigor Yang* and Fred E. C. Culick**
California Institute of Technology
Pasadena, California

ABSTRACT

Pressure oscillations in ramjet engines have been studied using an approximate method which treats the flow fields in the inlet and the combustor separately. The acoustic fields in the combustor are expressed as syntheses of coupled nonlinear oscillators corresponding to the acoustic modes of the chamber. The influences of the inlet flow appear in the admittance function at the inlet/combustor interface, providing the necessary boundary condition for calculation of the combustor flow. A general framework dealing with nonlinear multi-degree-of-freedom system has also been constructed to study the time evolution of each mode. Both linear and nonlinear stabilities are treated. The results obtained serves as a basis for investigating the existence and stabilities of limit cycles for acoustic modes. As a specific example, the analysis is applied to a problem of nonlinear transverse oscillations in ramjet engines.

1. INTRODUCTION

With the growing commitment to the development of ramjets and ducted rockets it has come to the recognition that instabilities within the propulsion system constitute a potential serious problem. This has been the subject of a JANNAF workshop reported in Ref. 1. Unsteady motions excited and sustained by the combustion processes are in fact a fundamental problem associated with any combustion chamber. The essential cause is the high rate of energy release confined to a volume in which energy losses are relatively small. Only a very small amount of chemical energy need be transformed to mechanical energy of time-varying fluid motions to produce unacceptably large excursion of pressure. The ensuing vibrations of the structure may lead to failure of the structure itself or of equipment and instrumentation.

Because the oscillations arise from causes entirely internal to the system, they are true instabilities and are correctly identified as self-excited. Typically, a small unstable initial disturbance will grow exponentially for some time, eventually reaching a limiting amplitude. This behavior necessarily involves nonlinear processes; it is impossible for an intrinsic instability to be limited by linear processes alone. Consequently, any question concerned with the long-time evolution of combustion instabilities can be addressed only by treatment of nonlinear processes. For ramjet engines, nonlinear behavior is especially concerned because of the difficulties in obtaining good quantitative data for the linear growth of oscillations. All information about combustion instabilities has been gained from observations of fully developed oscillations.

Figure 1 shows the situation examined here, an idealized representation of several contemporary ramjet engines using dump combustors. Air is delivered from a supersonic inlet system to a combustor in which chemical reaction takes place. Compared with rocket engines, ramjets have several characteristics which produce distinctive differences in the pressure oscillations observed. First, an important boundary condition is presented by the shock system located at the divergent section of the inlet diffuser. Second, combustion is confined to a chamber which is a substantial part but not the whole of the volume of the system. The inlet flow may play an important role in oscillations. The Mach number of the mean flow in the inlet can be quite high and should not be ignored, whereas the Mach number of the combustor flow is generally small. Third, the abrupt enlargement of cross-sectional area at the inlet/combustor interface produces recirculating flows and reacting turbulent shear layers, imposing serious difficulties in the theoretical modeling.

Several linear analyses of bulk and longitudinal oscillations in ramjets[2-5] have been developed, giving results valid in the limit of small amplitudes and low frequencies. Nonlinear analysis has not yet been accomplished although much of the necessary foundation is in place. Officially, two approaches can be followed: numerical techniques and approximate methods. Each approach has advantages which are complementary to the other. Numerical integration of the complete conservation equations provides more accurate and thorough results for well-posed problems; and serves as the only certain means of checking the validity of approximate methods. To date only longitudinal wave motions in solid propellant rockets have been treated successfully.[6] Extension to

---

*Research Fellow in Jet Propulsion, presently at The Pennsylvania State University, University Park, Pennsylvania.

**Professor of Applied Physics and Jet Propulsion.

multi-dimensional problems, especially for ramjet engines having non-uniform configuration, still remains in an early stage due to the complexity and uncertainty of the flowfield and the limitation of computer capability. An intrinsic disadvantage of numerical analysis is that the method yields one answer for each special case considered. Many cases must be run to detect trends and gain understanding. In contrast, approximate analysis provides more sweeping results less expensively and offers a framework for modeling physical behavior in a relatively easy manner. That is an attractive feature especially for studying mechanisms proposed as the causes of unsteady motions. In the work described herein, we are concerned only with an approximate analysis.

Because the characteristic features of the inlet and the combustor flows are basically different, for convenience of formulation they are treated separately. The flow in the inlet section downstream of the diffuser is taken to be uniform. We ignore the transverse wave motions since observations[7] have shown that the high frequency oscillations in the combustor do not transmit into the inlet as a consequence of the abrupt area change. Accordingly, the oscillatory field consists of two travelling waves. One is generated by the unsteady combustion processes in the combustor and propagates upstream; and the other is reflected downstream by the shock. Their influences on the combustor flow appears in the specification of the acoustic admittance function at the dump plane.

The flowfield in the combustor is much more complicated, usually involving both longitudinal and transverse wave motions.[7,8] Figure 2, the frequency content of pressure oscillations in a laboratory ramjet combustor operated at the Naval Weapons Center,[7] clearly demonstrates these two modes of instabilities. The basis for the analysis begins with an approximate method previously reported in Reference 9. The acoustic field is expressed as a synthesis of coupled nonlinear oscillators constructed in correspondence to the normal modes of the chamber. With application of the Galerkin method and the method of time averaging, a set of coupled first-order ordinary differential equations are obtained for the time evolution of each mode.

In the following sections, a formal framework for the nonlinear acoustic fields in ramjet engines is first constructed, followed by development of an approximate method dealing with nonlinear multi-degree-of-freedom system. The analysis serves as a basis for investigating the existence and stability of limit cycles for pressure oscillations. As a specific example, we treat a problem of nonlinear transverse wave motions for which the frequencies of the higher modes are not integral multiples of the fundamental frequency. This mode of oscillations has been previously studied by Zinn and Powell[10] for liquid propellant rockets. With the aid of the Galerkin method, they were able to derive a system of second-order ordinary differential equations governing the time-dependent amplitude of each mode, which were then solved numerically to predict the existence of limit cycles. Being different from their approach, it is intended in the present work to construct a realistic simple model so that explicit formulas can be obtained to explain some of the nonlinear behavior of engines.

2. ACOUSTIC FIELD IN THE INLET

To simplify the analysis, we ignore the cross-sectional area changes and assume the mean flowfield to be uniform. The rapid variations in the diffuser section appear indirectly through its influences on the boundary conditions. Therefore, we treat the problem of oscillatory motions in a uniform mean flowfield. Following the analysis given in Reference 11, we may express the linear acoustic pressure and velocity in the useful form

$$p_1' = P \exp\left[-i(\omega t + \bar{M}_1 Kx - \psi_p)\right] \tag{1}$$

$$u_1' = U \exp\left[-i(\omega t + \bar{M}_1 Kx - \psi_u)\right] \tag{2}$$

$$P = P_- \left[1 + |\beta|^2 + 2|\beta| \cos(2Kx + \phi)\right]^{1/2} \tag{3}$$

$$U = (1/\bar{\rho}_1 \bar{a}_1) P_- \left[1 + |\beta|^2 - 2|\beta| \cos\phi\right]^{1/2} \tag{4}$$

$$\tan\psi_p = \frac{-\sin Kx + |\beta| \sin(Kx + \phi)}{\cos Kx + |\beta| \cos x(Kx + \phi)} \tag{5}$$

$$\tan\psi_u = \frac{\sin Kx + |\beta| \sin(Kx + \phi)}{-\cos Kx + |\beta| \cos x(Kx + \phi)} \tag{6}$$

where K is the modified wave number defined as

$$K = \frac{k}{1-\bar{M}_1^2} = \frac{(\omega - i\alpha)/\bar{a}_1}{1-\bar{M}_1^2} \tag{7}$$

and β is $\exp(2iKL_1)$ times the acoustic reflection coefficient at the shock, $\beta = |\beta| \exp(i\phi)$.

It is clear that the acoustic field depends mainly on the reflection coefficient β, the Mach number $\bar{M}_1$, and the complex wave number K. For practical designs $|\beta|$ is very small, usually less than 0.1. Hence to first order accuracy of $|\beta|$, the acoustic admittance function at the upstream side of the dump plane ($x=0_-$) is

$$A_{d_1} = \left.\frac{\bar{\rho}_1 \bar{a}_1 u_1'}{p_1'}\right|_{x=0_-} = [1 - 2|\beta| \cos\phi] \exp[i(\psi_u - \psi_p)] \tag{8}$$

where

$$\psi_u - \psi_p = \tan^{-1}(-2|\beta| \sin\phi) \tag{9}$$

To check the validity of (8) and to show the dependence of A_{d_1} on the dimensionless frequency Ω, defined in Ref. 11, and wave number KL_1, some calculations based on (1)-(7) have been carried out with no approximation made. The results are given in Figure 3.

3. COUPLING OF THE INLET AND THE COMBUSTOR

The acoustic field in the combustor must be coupled to that in the inlet by requiring that the acoustic pressure and mass flux be continuous. Figure 4 shows the relevant notations. The conditions to be satisfied are

$$p_1' = p_2' \tag{10}$$

$$\bar{\rho}_1 u_1' + \rho_1' \bar{u}_1 = (\bar{\rho}_2 u_2' + \rho_2' \bar{u}_2) \frac{A_2}{A_1} \tag{11}$$

Assume isentropic condition at the dump plane,

$$\rho_1' = p_1'/\bar{a}_1^2 \quad ; \quad \rho_2' = p_2'/\bar{a}_2^2$$

Substitution of these equations into (11) and rearrangement of the result give the admittance function at the combustor side of the dump plane

$$A_{d_2} = \left.\frac{\bar{\rho}_2 \bar{a}_2 u_2'}{p_2'}\right|_{x=0_+} = (A_{d_1} + \bar{M}_1) \frac{\bar{a}_2}{\bar{a}_1} \frac{A_1}{A_2} - \bar{M}_2 \tag{12}$$

Combination of (8) and (12) yields

$$\text{real part of } A_{d_2} = (1-2|\beta| \cos\phi + \bar{M}_1) \frac{\bar{a}_2}{a_1} \frac{A_1}{A_2} - \bar{M}_2 + O(\beta^2) \tag{13}$$

$$\text{imaginary part of } A_{d_2} = -2|\beta| \sin\phi \frac{\bar{a}_2}{\bar{a}_1} \frac{A_1}{A_2} + O(\beta^2) \tag{14}$$

Because it is the imaginary part of A_{d_2} which determines the shift of frequency of oscillation from ω_n, the frequency of unperturbed normal mode, for small $|\beta|$ equation (14) implies that the acoustic mode shape in the combustor is very close to that in an organ pipe, as shown by recent experimental results.[7]

4. ACOUSTIC FIELD IN THE COMBUSTOR

The flow field in the combustor can be treated with the general analysis constructed in Reference 9. Briefly, the acoustic fields are synthesized as an expansion in normal modes,

following a procedure equivalent to the Galerkin method, or method of least residuals. Thus, the pressure and velocity fields are written:

$$p'(\vec{r},t) = \bar{P} \sum_i \eta_i(t)\, \psi_i(\vec{r}) \tag{15}$$

$$\vec{u}'(\vec{r},t) = \sum_i \frac{\dot{\eta}_i(t)}{\gamma k_i^2} \nabla\psi_i(\vec{r}) \tag{16}$$

where

$$\psi_i(\vec{r}) = \cos k_\ell x \cos m\theta\, J_m(k_j r), \quad \text{and} \quad k_i^2 = k_\ell^2 + k_j^2$$

These forms are substituted in the conservation equations expanded to second order in small quantities. Spacial averaging produces the set of equations representing a collection of coupled nonlinear oscillators:

$$\ddot{\eta}_n + \omega_n^2 \eta_n = \varepsilon F_n \tag{17}$$

where ε is a small parameter representing the amplitude of pressure oscillation, and F_n is the forcing function

$$F_n = -\sum_i \left[D_{ni}\dot{\eta}_i + E_{ni}\dot{\eta}_i\right] - \sum_i \sum_j \left[A_{nij}\dot{\eta}_i\dot{\eta}_j + B_{nij}\eta_i\eta_j\right] \tag{18}$$

The mathematical and physical meanings of the coefficients D_{ni}, etc., have been given in Ref. 9. Thus the problem comes down to solving the set (17) for the time-dependent amplitude, to give the evolution of the system subsequent to a specified initial condition.

4.1 Method of Time Averaging

We assume the solution to (17) has the form

$$\eta_n(t) = A_n(t)\sin\omega_n t + B_n(t)\cos\omega_n t \tag{19}$$

Imposing the condition

$$\dot{A}_n \sin\omega_n t + \dot{B}_n \cos\omega_n t = 0$$

and following some straightforward manipulation, we obtain the equations for $A_n(t)$ and $B_n(t)$.

$$\dot{A}_n = \frac{1}{\omega_n} \varepsilon F_n \cos\omega_n t \tag{20}$$

$$\dot{B}_n = \frac{-1}{\omega_n} \varepsilon F_n \sin\omega_n t \tag{21}$$

These equations (20) and (21) represent the exact solutions without any approximation made. To have a better understanding of A_n and B_n, we introduce two dimensionless time variables: the fast time τ_f and the slow time τ_s. Then equations (20) and (21) will generally contain terms of the form shown:

$$\frac{dA_n}{d\tau_s} = \frac{1}{\omega_n^2} F_n \cos\tau_f - f_o(\tau_s) f_1(\tau_f) + f_2(\tau_s) + f_3(\tau_f) \tag{22}$$

$$\frac{dB_n}{d\tau_s} = \frac{-1}{\omega_n^2} F_n \sin\tau_f - g_o(\tau_s) g_1(\tau_f) + g_2(\tau_s) + g_3(\tau_f) \tag{23}$$

where $\tau_s = \varepsilon\omega_n t$ and $\tau_f = \omega_n t$. The equations imply that A_n and B_n are slowly varying functions of time since τ_s represents the slowly varying time scale. For small τ_s and in the limit of $\varepsilon \to 0$, $\tau_f = \tau_s/\varepsilon \gg 1$. Thus $f_o(\tau_s)$ changes slightly while $f_1(\tau_f)$ may have experienced a considerable number of oscillations, as shown schematically in Figure 5. To a very good approximation, the fast varying functions $f_1(\tau_f)$ and $g_1(\tau_f)$ can be replaced by their time-mean quantities in the numerical integration for A_n and B_n. Therefore,

$$\frac{dA_n}{d\tau_s} \sim f_o(\tau_s) \langle f_1(\tau_f) \rangle + f_2(\tau_s) + \langle f_3(\tau_f) \rangle \tag{24}$$

$$\frac{dB_n}{d\tau_s} \sim g_o(\tau_s) \langle g_1(\tau_f) \rangle + g_2(\tau_s) + \langle g_3(\tau_f) \rangle \tag{25}$$

where

$$\langle f_1(\tau_f) \rangle = \frac{1}{T} \int_o^T f_1(\tau_f) d\tau_f, \quad T \to \infty \quad ; \quad \text{etc.}$$

$$\langle g_1(\tau_f) \rangle = \frac{1}{T} \int_o^T g_1(\tau_f) d\tau_f, \quad T \to \infty \quad ; \quad \text{etc.}$$

In summary, the method contains two steps: separation of the fast and the slowly varying terms; and time average of the fast varying terms. For some practical problems, there is no clear cut between the fast and the slowly varying terms. *An extensive numerical study has shown that* those terms with frequencies greater than one half of ω_n should be averaged with respect to time in order to have good approximation.

4.2 Linear Oscillation

The linear contribution to the forcing function F_n can be expressed as

$$(F_n)_{\text{linear}} = -\sum_i [D_{ni}\dot{\eta}_i + E_{ni}\eta_i] = -\sum_i [c_{ni}\cos\omega_i t + s_{ni}\omega_i t] \tag{26}$$

where

$$c_{ni} = \omega_i D_{ni} A_i + E_{ni} B_i \quad ; \quad s_{ni} = -\omega_i D_{ni} B_i + E_{ni} A_i$$

Substitution in (22) and (23) and neglect of the fast varying terms with frequencies $\omega_i + \omega_n$ give

$$\dot{A}_n = \frac{-1}{2\omega_n} \sum_i [c_{ni}\cos(\omega_i - \omega_n)t + s_{ni}\sin(\omega_i - \omega_n)t] \tag{27}$$

$$\dot{B}_n = \frac{1}{2\omega_n} \sum_i [-c_{ni}\sin(\omega_i - \omega_n)t + s_{ni}\cos(\omega_i - \omega_n)t] \tag{28}$$

Care must be exercised when dealing with terms with frequencies $\omega_i - \omega_n$. They are either fast or slowly varying, depending on the modes considered. We treat first the longitudinal mode of oscillation.

Longitudinal Modes - For practical ramjet engines with aspect ratio L/D greater than four, the longitudinal oscillations are linearly decoupled from the tangential and the radial modes as seen easily from the frequency difference. The coupling terms are fast varying and vanish after time averaging. For pure longitudinal modes, the terms survive only for i = n. Thus equations (27) and (28) become

$$\dot{A}_n = \frac{-1}{2\omega_n} c_{nn} = \frac{-1}{2\omega_n} [\omega_n D_{nn} A_n + E_{nn} B_n] \tag{29}$$

$$\dot{B}_n = \frac{1}{2\omega_n} s_{nn} = \frac{1}{2\omega_n} [-\omega_n D_{nn} B_n + E_{nn} A_n] \tag{30}$$

The linear coupling between pure longitudinal modes vanishes.

Tangential Modes - As discussed earlier, the frequency of the mixed longitudinal/tangential mode is

$$\omega_n = \sqrt{\omega_\ell^2 + \omega_j^2}$$

where ω_ℓ and ω_j stand for the frequencies of the pure longitudinal and tangential modes. In general, ω_ℓ is much less than ω_j for $\ell = 1,2$. If we let $\omega_\ell/\omega_j = \delta$, then

$$\omega_n = \omega_j [1 + O(\delta^2)]$$

The frequency difference between the pure tangential mode and the mixed mode is of second order in δ. Thus within first order accuracy,

$$\cos(\omega_n - \omega_i)t = 1 \quad ; \quad \sin(\omega_n - \omega_i)t = 0$$

The subscripts n and i denote the pure tangential mode and the mixed mode respectively, i = 1.2. Consequently, the equations governing linear tangential oscillations are

$$\dot{A}_n = \frac{-1}{2\omega_n} \sum_i c_{ni} = \frac{-1}{2\omega_n} \sum_i [\omega_i D_{ni} A_n + E_{ni} B_i] \tag{31}$$

$$\dot{B}_n = \frac{1}{2\omega_n} \sum_i s_{ni} = \frac{-1}{2\omega_n} \sum_i [\omega_n D_{ni} B_n - E_{ni} A_i] \tag{32}$$

The coefficients D_{ni} and E_{ni} are in general nonzero. Typically, they involve terms such as $\int \psi_i \vec{u} \cdot \nabla \psi_n dv$, which after some straightforward manipulations becomes

$$- \int \ell_i \bar{u}_x \cos\ell_n x \cos\ell_1 x [\cos i\theta J_i(k_1 r)]^2 dv.$$

The strong coupling between the tangential and the mixed modes indicates that the tangential oscillation depends greatly on the flow field in the axial direction[12], unlike the longitudinal mode which is relatively insensitive to the transverse flow motions.

Some calculations have been carried out for the transverse oscillations in a laboratory device operated at the Naval Weapons Center.[7] For simplicity, we consider only two modes with the mode shapes and the frequencies given below.

1st tangential mode $\psi_1 = \cos\theta J_1(k_1 r)$; $\omega_1 = 3816$ Hz

1st mixed mode $\psi_2 = \cos\left(\frac{\pi}{L} x\right)\cos\theta J_1(k_1 r)$; $\omega_2 = 3854$ Hz

Thus equations (31) and (32) give

$$\dot{A}_1 = \frac{-1}{2\omega_1}\left[\omega_1 D_{11} A_1 + E_{11} B_1 + \omega_2 D_{12} A_2 + E_{12} B_2\right] \tag{33a}$$

$$\dot{B}_1 = \frac{-1}{2\omega_1}\left[E_{11} A_1 - \omega_1 D_{11} B_1 + E_{12} A_2 - \omega_2 D_{12} B_2\right] \tag{33b}$$

$$\dot{A}_2 = \frac{-1}{2\omega_2}\left[\omega_1 D_{21} A_1 + E_{21} B_1 + \omega_2 D_{22} A_2 + E_{22} B_2\right] \tag{33c}$$

$$\dot{B}_2 = \frac{1}{2\omega_2}\left[E_{21} A_1 - \omega_1 D_{21} B_1 + E_{22} A_2 - \omega_2 D_{22} B_2\right] \tag{33d}$$

For convenience these equations can be written in matrix form, and the growth rates and the frequency shifts for linear oscillations are then easily determined by the eigenvalues of the coefficient, or augmentation, matrix.

Radial Modes - Similar to longitudinal motion, this mode of oscillation does not involve any significant linear coupling with the other modes and is not addressed here.

4.3 Nonlinear Oscillation

Following the same notations as those in Reference 9 and substituting (18) in (20) and (21), the equations governing the nonlinear oscillations can be written in the form

$$\dot{A}_n = \frac{-1}{2\omega_n}\sum_i \{c_{ni}[\cos(\omega_i - \omega_n)t + \cos(\omega_i + \omega_n)t] + s_{ni}[\sin(\omega_i - \omega_n)t + \sin(\omega_i - \omega_n)t]\}$$

$$- \frac{1}{2\omega_n}\sum_i \sum_j \{C_{nij} a_{ij}[\cos(\omega_n + \omega_+)t + \cos(\omega_n - \omega_+)t]$$

$$+ D_{nij} b_{ij}[\cos(\omega_n + \omega_-)t + \cos(\omega_n - \omega_-)t]$$

$$- C_{nij}c_{ij}[\sin(\omega_n + \omega_+)t + \sin(\omega_+ - \omega_n)t]$$

$$+ D_{nij}d_{ij}[\sin(\omega_n + \omega_-)t + \sin(\omega_- - \omega_n)t] \} \tag{34}$$

$$\dot{B}_n = \frac{1}{2\omega_n}\sum_i \{c_{ni}[\sin(\omega_n + \omega_i)t + \sin(\omega_n - \omega_i)t] + s_{ni}[\cos(\omega_i - \omega_n)t - \cos(\omega_i + \omega_n)t]\}$$

$$+ \frac{1}{2\omega_n}\sum_i\sum_j \{C_{nij}a_{ij}[\sin(\omega_n + \omega_+)t + \sin(\omega_n - \omega_+)t]$$

$$+ D_{nij}b_{ij}[\sin(\omega_n + \omega_-)t + \sin(\omega_n - \omega_-)t]$$

$$- C_{nij}c_{ij}[\cos(\omega_n - \omega_+)t - \cos(\omega_n + \omega_+)t]$$

$$+ D_{nij}d_{ij}[\cos(\omega_n - \omega_-)t - \cos(\omega_n + \omega_+)t] \} \tag{35}$$

where

$$\omega_+ = \omega_i + \omega_j \text{ ; and } \omega_- = \omega_i - \omega_j \tag{35}$$

The equations essentially contain two parts: coefficients arising from linear processes and nonlinear coupling among modes. For pure longitudinal oscillations for which the normal mode frequency is integral multiple of the fundamental frequency, $\omega_n = n\omega_1$, the analysis can be greatly simplified.[9] A detailed discussion of the stability and existence of the limit cycle has been given in Reference 13. The influences of tangential oscillations on longitudinal motions are generally small except for a short combustor having low aspect ratio, as seen easily from the frequency components.

$$\frac{\omega_n - \omega_+}{\omega_n}, \quad \frac{\omega_n - \omega_-}{\omega_n}, \quad \frac{\omega_n + \omega_+}{\omega_n}, \quad \frac{\omega_n + \omega_-}{\omega_n} \neq 0\ (\delta)$$

Tangential modes are commonly observed in many ramjet combustors.[7,8] As a first approach, we consider only two modes here: the first tangential and radial modes. The coupling with the mixed longitudinal/tangential modes and the higher tangential modes are not included, but can be treated in the same manner. Following the same idea discussed earlier, the fast varying terms are averaged with respect to time. Thus, equations (34) and (35) become:

$$\dot{A}_1 = \alpha_1 A_1 + \theta_1 B_1 + a[(A_1A_2 + B_1B_2)\cos\Omega t - (A_2B_1 - A_1B_2)\sin\Omega t] \tag{36}$$

$$\dot{B}_1 = \alpha_1 B_1 - \theta_1 A_1 - a[(A_1A_2 + B_1B_2)\sin\Omega t + (A_2B_1 - A_1B_2)\cos\Omega t] \tag{37}$$

$$\dot{A}_2 = \alpha_2 A_2 + \theta_2 B_2 + b[(A_1^2 - B_1^2)\cos\Omega t - 2A_1A_2\sin\Omega t] \tag{38}$$

$$\dot{B}_2 = \alpha_2 B_2 - \theta_2 A_2 + b[(A_1^2 - B_1^2)\sin\Omega t + 2A_1 B_1 \cos\Omega t] \tag{39}$$

where $\Omega = 2\omega_1 - \omega_2$, and α_i, θ_i, a, and b are coefficients arising from linear and nonlinear processes. They are defined as

$$\alpha_1 = -\frac{D_{11}}{2} \; ; \quad \theta_1 = -\frac{E_{11}}{2\omega_1} \; ; \quad a = -\frac{D_{112}}{4\omega_1} - \frac{D_{121}}{4\omega_1}$$

$$\alpha_2 = -\frac{D_{22}}{2} \; ; \quad \theta_2 = -\frac{E_{22}}{2\omega_2} \; ; \quad b = -\frac{C_{211}}{4\omega_2}$$

To obtain results for periodic limit cycles, we look for the limiting values of A_i and B_i (i = 1,2) in the following form.

$$\begin{aligned} A_1 &= r_1\cos(\theta t + \nu_1) \\ B_1 &= r_1\sin(\theta t + \nu_1) \\ A_2 &= r_2\cos(\theta t + \nu_2) \\ B_2 &= r_2\sin(\theta t + \nu_2) \end{aligned} \tag{40}$$

Substitution in (36) through (39) and rearrangement of the results yield

$$-r_1\theta\sin(\theta t + \nu_1) = r_1\sqrt{\alpha_1^2 + \theta_1^2}\cos(\theta t + \nu_1 - \psi_1) + ar_1r_2\cos(\Omega t + \nu_1 - \nu_2) \tag{41}$$

$$r_1\theta\cos(\theta t + \nu_1) = r_1\sqrt{\alpha_1^2 + \theta_1^2}\sin(\theta t + \nu_1 - \psi_1) - ar_1r_2\sin(\Omega t + \nu_1 - \nu_2) \tag{42}$$

$$-r_2\theta\sin(\theta t + \nu_2) = r_2\sqrt{\alpha_2^2 + \theta_2^2}\cos(\theta t + \nu_2 - \psi_2) + br_1^2\cos(2\theta t + \Omega t + 2\nu_1) \tag{43}$$

$$r_2\theta\cos(\theta t + \nu_2) = r_2\sqrt{\alpha_2^2 + \theta_2^2}\sin(\theta t + \nu_2 - \psi_2) + br_1^2\sin(2\theta t + \Omega t + 2\nu_1) \tag{44}$$

where

$\psi_1 = \tan^{-1}\frac{\theta_1}{\alpha_1}$; $\psi_2 = \tan^{-1}\frac{\theta_2}{\alpha_2}$. Clearly, the solutions exist only if $\theta = -\Omega$.

To equate the time-dependent terms on both sides of the above equation, we find $\theta = -\Omega$. Now multiply equation (41) by $\sin(\Omega t - \nu_1)$, (42) by $\cos(\Omega t - \nu_1)$ and subtract to find

$$\Omega - \theta_1 - ar_2\sin(2\nu_1 - \nu_2) = 0 \tag{45}$$

Multiply equation (41) by $\cos(\Omega t - \nu_t)$, (42) by $\sin(\Omega t - \nu_1)$ and add to find

$$\alpha_1 + ar_2\cos(2\nu_1 - \nu_2) = 0 \tag{46}$$

Similar manipulations of equations (43) and (44) give

$$\gamma_2(\Omega - \theta_2) + b\gamma_1^2 \sin(2\nu_1 - \nu_2) = 0 \tag{47}$$

$$\alpha_2\gamma_2 + b\gamma_1^2 \cos(2\nu_1 - \nu_2) = 0 \tag{48}$$

Equations (46) and (48) give

$$\gamma_1^2 = \frac{-\alpha_1\alpha_2}{ab} \frac{1}{\cos^2(2\nu_1 - \nu_2)} \tag{49}$$

Since ab is positive, the sufficient and necessary condition for the existence of limit cycle is

$$\alpha_1\alpha_2 < 0 \tag{50}$$

The time evolution of the acoustic mode is obtained by substituting (40) in (19). Thus,

$$\eta_1(t) = \gamma_1 \sin(\omega_1 t + \theta t + \nu_1)$$

$$\eta_2(t) = \gamma_2 \sin(\omega_2 t + \theta t + \nu_2)$$

Since $\theta = -\Omega = \omega_2 - 2\omega_1$, we have

$$\eta_1(t) = \gamma_1 \sin[(\omega_2 - \omega_1)t + \nu_1]$$

$$\eta_2(t) = \gamma_2 \sin[2(\omega_2 - \omega_1)t + \nu_2]$$

The frequency of the first radial mode is twice of that of the first tangential mode as a result of nonlinear coupling.

CONCLUSION REMARKS

A general framework for studying pressure oscillations in ramjet engines has been constructed. The method extended previous analysis of nonlinear acoustics so that results can be obtained for cases in which the linear normal modes are not simply organ pipe modes. The analysis of existence of limit cycles for transverse acoustic modes has also been carried out with only two modes taken into account. The cases for three and more modes will be discussed in subsequent work.

ACKNOWLEDGMENTS

This work was supported partly by the California Institute of Technology, and partly by the Department of the Navy, ONR Contract N00014-84-K-0434.

REFERENCES

1. Culick, F. E. C., "Report of the JANNAF Workshop on Pressure Oscillations in Ramjets," 1980 JANNAF Propulsion Meeting; Seventeenth JANNAF Combustion Meeting, 1980.

2. Culick, F. E. C. and Rogers, T., "Modeling of Pressure Oscillations in Ramjets," AIAA/SAE/ASME Sixteenth Joint Propulsion Conference, 1980.

3. Yang, V. and Culick, F. E. C., "Analysis of Low Frequency Combustion Instabilities in a Laboratory Ramjet Combustor," Combustion Science and Technology, October 1985 (to be published).

4. Reardon, F. H., "The Sensitive Time Lag Model Applied to Very Low Frequency Oscillations in Side-Dump Liquid-Fueled Ramjet Engines," Twentieth JANNAF Combustion Meeting, 1983.

5. Abouseif, G. E., Keklak, J. A., and Toong, T. Y., "Ramjet Ramble: The Low Frequency Instability Mechanism in Coaxial Dump Combustor," Combustion Science and Technology, Vol. 36, 1984, p. 83.

6. Baum, J. D. and Levine, J. N., "Evaluation of Finite Difference Schemes for Solving Nonlinear Wave Propagation in Rocket Combustion Chambers," AIAA Paper No. 81-0420, 1981.

7. Crump, J. E., Schadow, K. C., Yang, V., and Culick, F. E. C., "Longitudinal Combustion Instabilities in Ramjet Engines: Identification of Acoustic Modes," accepted for publication in AIAA Journal of Propulsion and Power.

8. Clark, W. H., "Geometric Scale Effects on Combustion Instabilities in a Side-Dump Liquid Fuel Ramjet," Nineteenth JANNAF Combustion Meeting, 1982.

9. Culick, F. E. C., "Nonlinear Behavior of Acoustic Waves in Combustion Chambers," Acta Astronautics, Vol. 3, No. 9, 1976, pp. 715-756.

10. Zinn, B. T. and Powell, E. A., "Nonlinear Combustion Instability in Liquid Propellant Rocket Engines," Thirteenth Symposium (International) on Combustion, The Combustion Institute, pp. 491-503.

11. Culick, F. E. C. and Rogers, T., "The Response of Normal Shocks in Diffusers," AIAA Journal, Vol. 21, 1983, pp. 1382-1390.

12. Reardon, F. H., "An Investigation of Transverse Mode Combustion Instability in Liquid Propellant Rocket Motors," Princeton University Aeronautical Engineering Report 550, June 1961.

13. Awad, E. and Culick, F. E. C., "On the Existence and Stability of Limit Cycles for Longitudinal Acoustic Modes in a Combustion Chamber," submitted to Combustion and Science for publication.

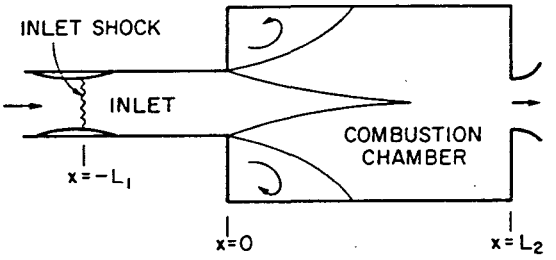

Fig. 1. Schematic Diagram of Ramjet Engine

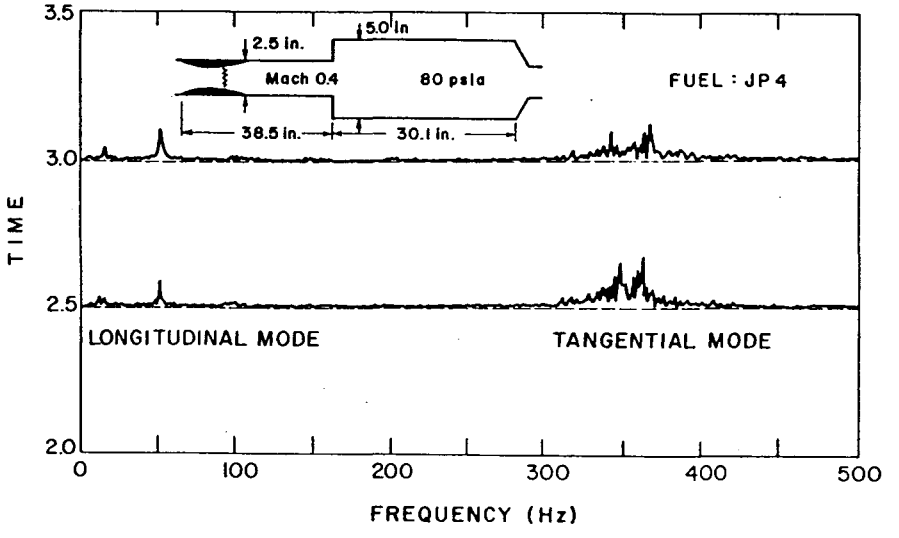

Fig. 2. Frequency Content of Pressure Oscillations in a Laboratory Ramjet Combustor[7]

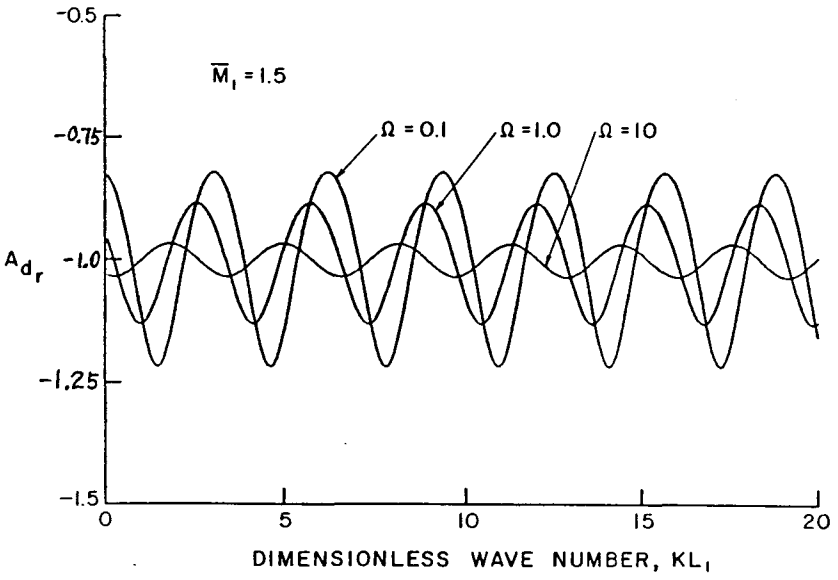

Fig. 3a. Real Part of Acoustic Admittance Function at the Inlet Side of the Dump Plane (x = 0_)

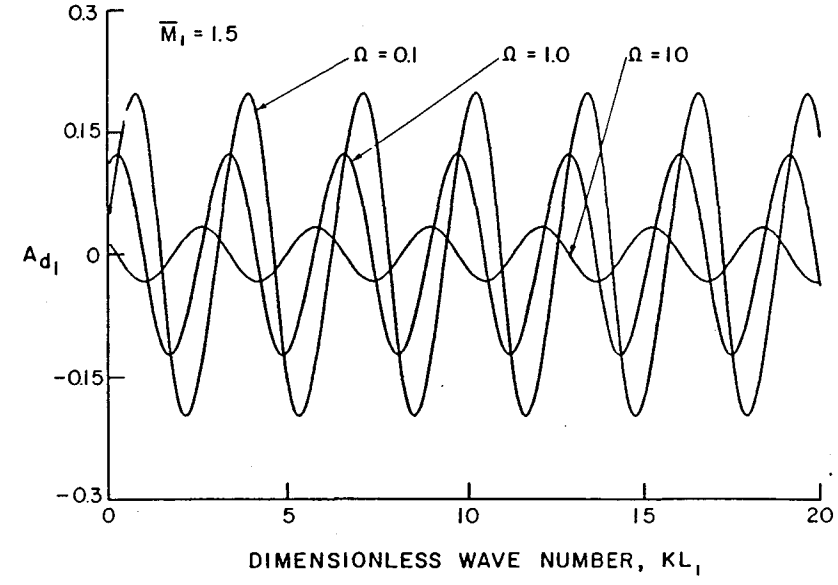

Fig. 3b. Imaginary Part of Acoustic Admittance Function at the Inlet Side of the Dump Plane (x = 0_)

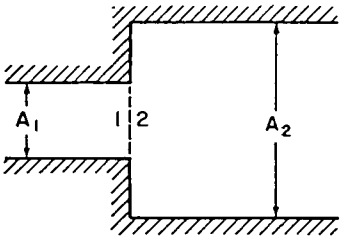

Fig. 4. Interface Between Inlet and Combustor

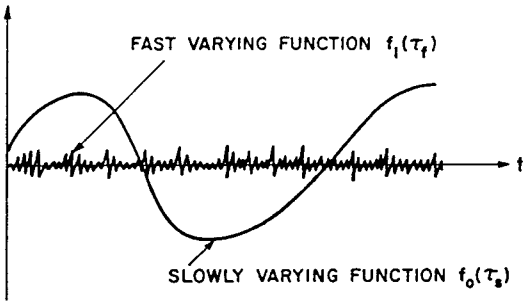

Fig. 5. Schematic Diagram of Fast and Slowly Varying Functions